

PROTOTYPE OF EUTECTIC REFRIGERATION SYSTEM WORKING WITH R1270 REFRIGERANT

Liutauras Vaitkus^(a), Lukas Prakopavičius^(a)

(a) Kaunas University of Technology, K. Donelaicio g. 73, Kaunas, LT-44029, Lithuania
e-mail: liutauras.vaitkus@ktu.lt (L. Vaitkus), lukas.prakopavicius@ktu.edu (L. Prakopavičius),

ABSTRACT

The new European F-Gas and PFAS Directives further reduce the availability of synthetic refrigerants. This article examines eutectic refrigerating systems used in weight-optimized low-temperature transport refrigerators for retail distribution. Such systems today use R452A with GWP=2140, and there are no suitable low GWP synthetic alternatives - transition to natural refrigerants could be the only option. This article examines a prototype eutectic refrigeration system with R1270. At the beginning the article briefly describes the working temperature regime of the eutectic refrigeration system, as well as the limiting factors. The early prototype was tested with R290 and R1270 refrigerants. The test results were considered when developing the second prototype. To further reduce refrigerant charge, thermal and hydraulic modelling of the evaporator (eutectic plates) was performed. At the end of the pull-down cycle, the evaporation pressure in the evaporator is in vacuum, therefore the control system has been developed to detect a possible leak on the low-pressure side. Test results of the second prototype are also presented.

Keywords: Eutectic refrigerating system, R1270 refrigerant test results, Refrigerant charge minimization.

1. INTRODUCTION

According to final text of the new Regulation EU573/2024 on fluorinated greenhouse gases, the quota for placing hydrofluorocarbons on the market for the 2030–2032-year period is reduced by almost $\frac{3}{4}$ - 5.2% from the 2015 level, instead of 21% according to Directive EU517/2014. This article is focused on the transport refrigerators (refrigerated light-duty vehicles) with a eutectic refrigerating system (ERS), which are used for the retail distribution of frozen food. In this application the number of destination points is high, and the driving time is insufficient for compensation of the heat intake during the distribution, therefore some form of accumulation is required. ERS uses a eutectic solution (phase change material) to store energy and is charged at night on mains power. Once the system is charged, it provides cooling for a specific duration of time.

The refrigerated light-duty vehicles are sensitive to the weight of the refrigerating system (mass of the fully loaded vehicle must not exceed 3500 kg). To decrease mass of ERS the refrigerated goods are often supercooled during the charging stage to store up to 50% of total accumulated energy. To supercool the products, the evaporation temperature at the end of pull-down cycle must be low, and may reach -60 °C. Such systems were traditionally used with the R404A or R507A refrigerants, and now are often used with R542A (GWP=2140), so the quota reduction of the new Directive will make these systems impractical. A eutectic refrigeration system capable of working with natural refrigerants needs to be developed.

Publications on transport refrigerators with an ERS are rare. Theoretical analysis and operating conditions of ERS as well as drop-in results with R418A and R452A are given respectively in Vaitkus and Dagilis (2017a) and Vaitkus and Balčius (2022). The traditional ERS is analysed by Vaitkus and Dagilis (2014). The main limiting factor with alternative refrigerants is the low evaporation pressure. Here we analyse a prototype of eutectic refrigeration system (ERS), which uses propylene as the refrigerant. With R1270 refrigerant, the eutectic plates can be crystallized when the evaporation pressure is higher than 1 bar (abs), but there will be a vacuum in the evaporator at the end of the charging cycle.

The article is organized as follows. Section 2 gives a brief description of the ERS and summarizes the results of

the first prototype with R1270, which was discussed in Vaitkus et al. (2024). In this paper, we present the second prototype, which is designed based on the test results of the first prototype. We focus on the major design change - the newly designed evaporator (eutectic plate) system. The calculations of eutectic plates are presented in Section 3. Section 4 presents some preliminary test results. Section 5 gives conclusions of the research.

2. FIRST ERS PROTOTYPE WITH R1270 - SUMMARY

The first ERS prototype was built for the low refrigerant charge, according to the principles described in Vaitkus and Dagilis (2014). It used a mini-channel low-volume condenser and receiver (with volume ~40% compared to baseline system). The mechanical crankcase pressure regulating valve (CPRV) was replaced with the MOP function of the EEV controller. However, the eutectic plate system of the first prototype was not optimized for low charge - the system consisted of two branches, their lengths are about 26.6 m and 33.3 m, the inner diameter of the tube is 13 mm. Accordingly, the total internal volume of the evaporator tube is approximately equal to 8 litres.

The system was equipped with suction – liquid heat exchanger (SLHX) with effectiveness ~73%. The effect of SLHX on the operation of refrigeration systems is studied in detail by Klein et.al., (2000). With hydrocarbons the use of SLHX increases the efficiency of the refrigerating system, but the temperature of the vapor in the suction line also increases, which may result in inadequate cooling of the compressor. Due to high compression ratio in ERS, the excessively high discharge temperature has a negative impact on durability of compressor and may become a limiting factor. In the second prototype the effectiveness of SLHX was reduced, and the system was equipped with economizer (the eutectic system with an economizer is described in Vaitkus and Dagilis, (2017b).

The first prototype was designed for R290 refrigerant but was also tested with R1270. Since the specific refrigerating capacity (heat absorbed in evaporator for one cubic meter of vapor at suction conditions) of the R1270 refrigerant under the conditions of the eutectic refrigeration system is about 24% higher compared to R290 (808.22 and 651.36 kJ/m³ for R1270 and R290 respectively), the displacement of the compressor was too high for R1270. Compared to the baseline R452A system, the displacement ratio of the first and second prototypes was 1.24 and 0.91, respectively. The minimum refrigerant charge measured for the first prototype was 750 g.

For the second prototype the focus was on reducing the refrigerant charge in evaporator. Although DIN EN 17893 does not define the maximum charge of the refrigerant, the maximum concentration of the refrigerant in the refrigerated body (in case of leakage) must not exceed 0.25 LFL. The amount of leakage into the refrigerated body depends on the refrigerant charge in the evaporator. The second prototype introduces a new configuration of evaporator (eutectic plates) with lower volume, but it should also ensure acceptable pressure losses and sufficiently efficient heat transfer. This prototype was built for the smaller displacement compressor. The calculation results of the new eutectic plates are presented in the next section.

3. CALCULATIONS OF NEW EUTECTIC PLATES

The calculations were performed for nominal operating conditions - evaporation and condensing temperatures -42 and 27 °C respectively, the effectiveness of SLHX 30%, with 0 K subcooling in condenser. The liquid refrigerant after condenser is subcooled in the economizer (10 K subcooling assumed), the superheat in the evaporator is 6 K, and the unusefull superheat in the suction line is 1 K. Compressor volumetric capacity assumed 6.7 m³/h. The calculated refrigerating capacity of the compressor is 1669 W, the mass flow rate is 5.18 g/s, the vapor quality at the evaporator inlet is 0.27 kg/kg. The vapor temperature at the compressor suction line is -19.4 °C, and the vapor temperature at the end of isentropic compression is 69.4 °C (about 128 °C for a realistic isentropic efficiency). In the baseline model with R452A (for the same evaporation and condensing temperatures) the temperature at the end of isentropic compression was higher by about 20 K (92.0 °C).

Heat transfer in evaporator was calculated using a diabatic two-phase flow pattern map and heat transfer model by Wojtan et. al., (2005a, 2005b). The hydraulic losses were calculated using mathematical model by Quibén et al., (2007a, 2007b), based on the same diabatic two-phase flow pattern map. Both mathematical models use the Steiner (1993) version of the Rouhani–Axelsson drift flux model for horizontal tubes for the cross-sectional void fraction. This drift flux void fraction model gives the void fraction as an explicit function of total mass flux. These models

use as input data 1) vapor quality at evaporator inlet (kg/kg), 2) mass velocity (kg/(m² s) (ratio of mass flow rate and pipe cross-sectional area), 3) pipe diameter (m), 4) heat flux (W/m²) (heat rate ratio with heat transfer area) and 5) evaporation temperature. The properties of the working fluid used in the mathematical model (saturation pressure, saturated liquid and vapor density, enthalpy, isobaric specific heat, dynamic viscosity, thermal conductivity, surface tension, critical pressure, and molar mass) are taken from Lemmon et.al., (2018). The initial data and results of the calculation of eutectic plates are presented in Table 1.

Table 1. Initial data and results of calculation of eutectic plates

Parameter and units	Baseline	Plate 1-4	Plate 5
Pipe internal diameter with respect to baseline system d/d_{bas} , [m/m]	1	0.615	1.23
Branch length with respect to long branch of baseline system, L/L_{bas} , [m/m]	1	0.4	0.2
Heat transfer area with respect to long branch of baseline system, A/A_{bas} , [m/m]	1	0.246	0.246
Vapor quality at evaporator inlet, [kg/kg]	0.27	0.27	0.9
Mass velocity, [kg/(m ² s)]	21.7	25.7	25.7
Heat flux, [W/m ²]	682.	1107	554
Evaporation temperature, [°C]	-42	-42	-42
Mean surface heat transfer coefficient, [W/(m ² K)]	281	412	380
Mean value of pressure gradient, [Pa/m]	121.4	358	176
Pressure drop in the evaporator, [Pa]	4043	4778	1174
The temperature difference corresponding to the pressure drop in the evaporator, K	0.73	0.87	0.21
Calculated temperature at the reference surface, [°C]	-39.56	-38.6	-40.5
Calculated temperature rise due to thermal resistance, [K]	2.24	3.4	1.5
The overall increase in temperature, [K]	2.97	4.27	1.7
Average “density” $(dM/dV)_m$, [kg/m ³]	39.40	42.47	8.53
Calculated refrigerant mass, kg	0.314	0.114	0.011

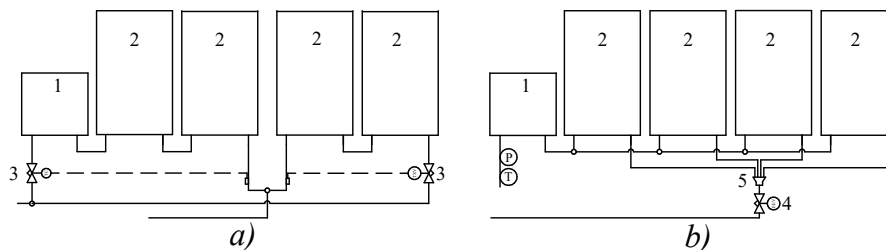


Fig. 1 Eutectic plate setup in a) baseline and b) prototype 2 systems; 1, 2 – eutectic plates, 3 – TXV, 4 – EEV, 5 – distributor, P, T – pressure and temperature sensors

In the Baseline model, the evaporator comprises two asymmetric branches connected in parallel, the length of the tube for the shorter and longer branches respectively is 2/4.5 and 2.5/4.5 of total length (see Fig.1). For calculations of the long branch the refrigerating capacity and mass flow rate were multiplied by 2.5/4.5. It is assumed that dry saturated vapor comes out of the evaporator. According to calculations, the flow pattern is stratified – wavy. The intensity of heat transfer is low - the mean heat transfer coefficient is just 280.7 W/m² K. The mean value of the pressure gradient is 121.4 Pa/m. The pressure drop in the evaporator is calculated as the product of the mean pressure gradient and the tube length and is equal to 4043 Pa (corresponds to 0.73 K temperature drop). The pressure drop calculated for the baseline system with R507A was equivalent to 1.39 K.

The evaporator volume of the Baseline system (~8 liters) must be reduced when designing a low-charge system. Simply reducing the diameter of the evaporator tube is not a viable option, because the pressure losses in the evaporator increases rapidly. For example, if we reduce the inner diameter of the pipe to diameter $d/d_{bas} = 0.77$, the drop in evaporation temperature due to hydraulic losses would increase from 0.73 to 3.2 K. The total drop in evaporation temperature would be slightly less than 2 K, which corresponds to about 5 % lower COP.

The diameter of the tube could be reduced while increasing the number of parallel branches. Such a setup could use a single EEV and supply the refrigerant to individual branches through a distributor. However, in the ERS it

is impossible to ensure structurally symmetrical branches nor symmetrical loading under real operating conditions. For the second R1270 prototype, we chose a combined evaporator setup - four structurally identical evaporator branches are connected in parallel and fed through one EEV and distributor, and then the entire flow converges into one and is fed to a serially connected plate. In the simulation, we assume that the eutectic plate connected in series will make 1/9 of the total eutectic liquid (and thermal load). The four parallel branches are symmetrical, and each is 2/9 of the thermal load. The mass flow rate of each parallel branch is 1/4 of the total mass flow rate, and the last plate has the full mass flow rate.

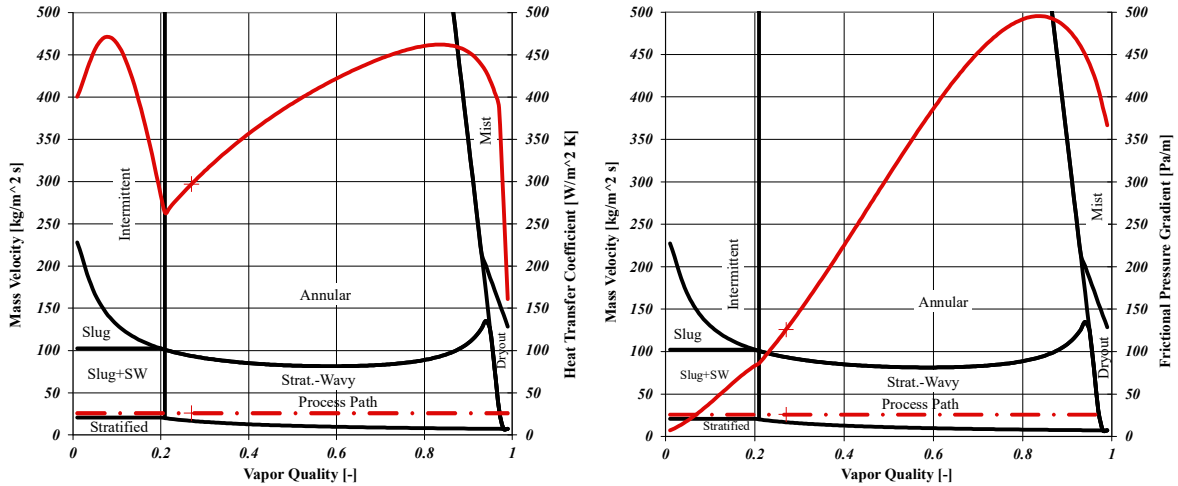


Fig. 2 Diabatic two-phase flow pattern map, heat transfer coefficient and frictional pressure gradient in the parallel plates (N1 to N4) of new evaporator

The calculation results of the new configuration of the evaporator are presented in Figure 2 and in Table 1 (separately for series- and parallel-connected sections). The flow mode in the new configuration evaporator remains stratified - wavy, but the intensity of heat transfer increases: in the part of parallel connected plates, the average heat transfer coefficient increases by 47%, and even in the serially connected part, where dryout takes place, the heat transfer coefficient is higher by about 35%. The total pressure drop (in parallel and series sections) is equivalent to a boiling temperature drop of 1.08 K.

When comparing the heat exchange efficiency, the temperature T_{S2} on the outer surface of the evaporator tube was calculated for the baseline system (see Fig.3a). This temperature is compared to the temperature at the same distance from the centre of the tube as the outer surface of the tube in the baseline systems. In Fig.3b, this would be the temperature T_{S2} at a distance r_3 from the centre of the tube, respectively. The thermal conductivity coefficient of the wall (steel) is taken as 42.5 W/mK, ice - 2.63 W/mK. The wall thickness in all cases is 1 mm.

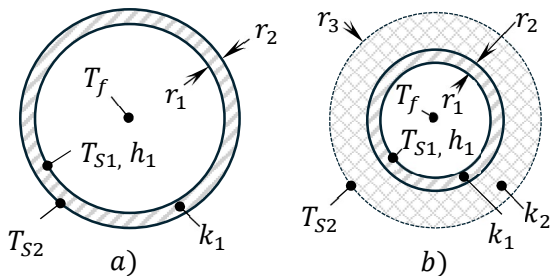


Fig. 3 Diagram for comparison of heat transfer through the wall in the evaporator: a) baseline system, b) new system

brackets is not evaluated.

For eutectic plates of parallel connected sections with a tube diameter smaller than the baseline system, the temperature T_{S2} is calculated according to the following formula:

$$T_{S2} = T_f + q \left(\frac{1}{2\pi r_1 L h_1} + \frac{\ln \frac{r_2}{r_1}}{2\pi L k_1} + \frac{\ln \frac{r_3}{r_2}}{2\pi L k_2} \right)$$

Where T_f – evaporation temperature, °C, q – heat rate, W, r_1, r_2, r_3 – respectively internal and external radius of pipe and radius of reference surface, m, L – length of pipe, m, k_1, k_2 – thermal conductivity of steel and ice respectively, W/mK, h_1 – mean surface heat transfer coefficient, W/m²K. For the baseline system (Fig. 4a) the third member in

The temperature of the reference surface for the plates connected in parallel was found to be about 1 K higher than in baseline system. This means that losses increase, and the evaporation temperature should decrease. However, this heat loss calculation is simplified - a significant part of the heat flow is transmitted through the wall of the eutectic plate – the wall works as a fin (extended surface).

The refrigerant charge is calculated according to the following formula:

$$M = \int_0^V [\varepsilon_v \rho_g + (1 - \varepsilon_v) \rho_f] dV$$

Where M – refrigerant charge, kg, ε_v - Rouhani–Axelsson void fraction, ρ_g, ρ_f – density of dry saturated vapor and saturated liquid respectively, kg/m³, V – evaporators volume, m³. The expression in the integral has units of density. Its average value in Table 1 is called "density". This value depends relatively little on the configuration of the evaporator (in both cases the mass velocity values are similar). At the same evaporation temperature (for a given refrigerant) the charge is essentially determined by the volume of the evaporator. The new configuration allows the calculated refrigerant charge in the evaporator to be reduced from 314 g to 125 g.

It should be noted here that the serially connected eutectic plate with $d/d_{bas} = 1.23$ could not be manufactured in time due to technological challenges, so the tested prototype had this plate with $d/d_{bas} = 1$. The test results are given in the next chapter.

4. PRELIMINARY TEST RESULTS OF THE SECOND PROTOTYPE

During the tests, the Iotech Personal Daq/56 Data acquisition module was used. Temperature was measured using K-type thermocouples, pressure - using Danfoss AKS 32 pressure transmitters. The ambient and inside air temperatures are an average of four and five points, respectively. Condensing and evaporation temperatures were calculated from corresponding pressures.

Table 2. Characteristics and uncertainty of measurement

Measurement	Probe and instrument	Accuracy	Uncertainty
Temperature	K-type thermocouple, Iotech pDaq/56	±0.17 K error (calibrated), 0.033 K STD 0.5 K cold junction compensation error	±1.06 K (at -33 °C)
Pressure	Danfoss pressure transducer AKS-32	Non-linearity BFSL - < ± 0.2% FS Hysteresis and repeatability - ≤ ± 0.1% FS Thermal zero-point shift - ≤ ± 0.2% FS / 10K Thermal span shift - ≤ ± 0.2% FS / 10K	±3.83 kPa for evap. pr. ±14.4 kPa for cond. pr.
Pull-down duration			±3.2%

The purpose of the initial tests was to evaluate the overall functionality. The biggest change was the new configuration of the evaporator. The parallel connection of evaporator branches requires symmetrical branches and symmetrical load. Such connection is common in forced convection air coolers. It is not clear how effective such a system is in ERS, where asymmetric loading can be expected, especially during refreezing.

The indicators measured during the initial tests were a) evaporation temperature during crystallization of the eutectic plates (compared to the first prototype), b) pull-down duration (compared to the first prototype), c) uniformity of freezing of parallel connected eutectic plates during freezing (without products), d) uniformity of freezing of parallel connected eutectic plates during refreezing after simulated distribution cycle (with products).

In Fig. 4 we see the average temperatures of the internal air, eutectic plates, and evaporation during pull-down at an ambient temperature of 27 °C. At the end of the pull-down estimation range (when the internal air temperature reaches -34 °C), the average temperature of the eutectic plates (midpoint) reached -44 °C, and evaporation temperature was still higher than -47.9 °C. Using R1270 the eutectic plates mostly finish crystallizing when the evaporation pressure does not yet go to vacuum (the eutectic liquid finishes crystallization at ~ -41 °C).

The evaporation temperature during crystallization of the eutectic plates was calculated from the time, inside air

and evaporation temperature data. The range of inside air temperature from -20 to -34 °C was divided into steps of 0.25 K, calculating duration to decrease the temperature each step. The relationship of such duration to inside air temperature is shown in Fig. 5. The interval of maximum cooling duration and the average evaporating temperature in this interval were then found. This evaporation temperature depends on several factors, such as the refrigerating capacity of the compressor, hydraulic losses in the evaporator and suction line, thermal losses in the eutectic plates and even the insulation quality of the isothermal body. Both prototypes were tested in the same isothermal body and the same eutectic liquid.

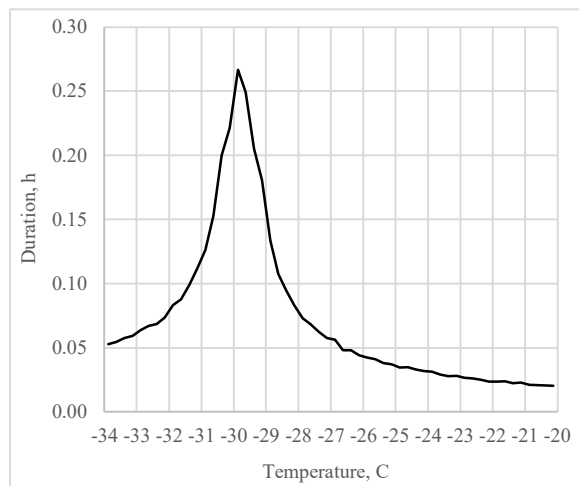
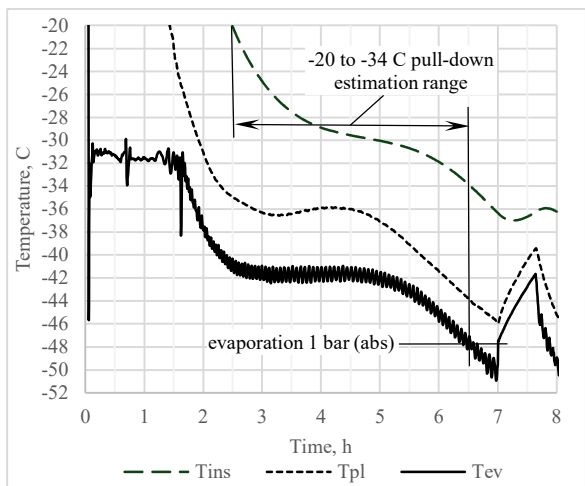


Fig. 4 Pull-down performance at 27 °C; T_{ins} – average inside air temp., T_{pl} – average eutectic plate temp., T_{ev} – evaporation temp. **Fig. 5** Duration of average inside air temperature drop of 0.25 K at 27 °C ambient temperature.

Fig. 6 gives the pull-down duration as a function of ambient temperature for both prototypes. Comparing to the first prototype, the compressor displacement of the second prototype is significantly lower (respectively 9.95 and 7.31 m³/h at 50 Hz), so the pull-down duration was expected to be longer, but the measured pull-down duration increase at 20 °C ambient temperature was less than 5%. Such high refrigerating capacity can be explained by the significantly higher subcooling of the liquid in the economizer - instead of the expected 10 K, a subcooling of almost 40 K was obtained. The first prototype was not equipped with an economizer.

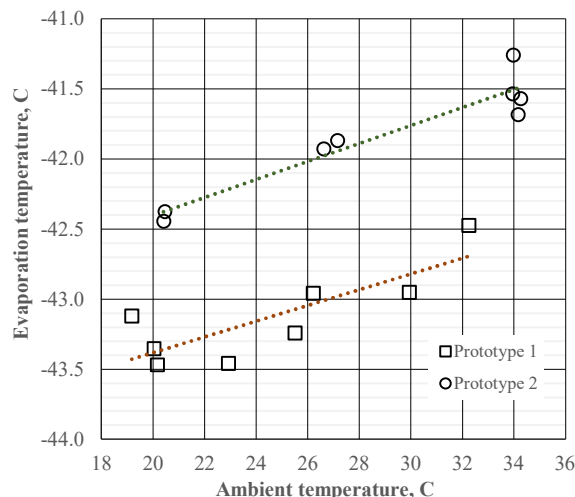
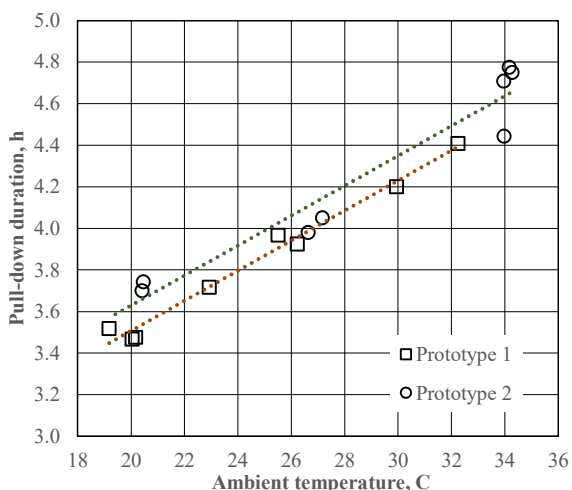


Fig. 6 The pull-down duration of eutectic systems from -20 to -34 °C inside air temperature at different ambient temperatures. **Fig. 7** Evaporation temperature during the crystallization of eutectic plates at different ambient temperatures.

Fig. 7 gives a comparison of evaporation temperatures as a function of ambient temperature for both prototypes. In the eutectic plates of the second prototype, a significantly smaller diameter tube was used, which reduced the heat transfer area from the refrigerant side. Nevertheless, the evaporation temperature increased by about 1 K, indicating lower overall losses in the eutectic plates. In both cases the refrigerating capacity of the compressors is almost the same, which is confirmed by the very close pull-down duration.

Fig.8 shows the eutectic plates temperature near exit during cooling of empty body after defrosting. As can be seen, all four eutectic plates connected in parallel and fed through the distributor cooled down almost at the same time, and their temperatures at the end of the pull-down estimation range are essentially the same. The fifth, serially connected eutectic plate, is delayed. In this plate, the superheating of the refrigerant occurs, the vapor temperature of the refrigerant increases, and heat transfer coefficient from the side of the refrigerant decreases. The delay in crystallization of the last (in the branch) eutectic plate is not unique to this system - in the baseline system (and in the first prototype) the delayed crystallization of the eutectic plates at the exit of both branches was observed.

Fig.9 shows the eutectic plates temperature near exit during cooling of loaded body during refreezing after the simulated sales cycle. The body was loaded with about 800 kg of wet (frozen) sawdust packages. The simulated sales cycle consisted of 90 door openings of 30 seconds each, for a total of 45 minutes with (one) door open. The test was carried out at an ambient temperature of 20 C.

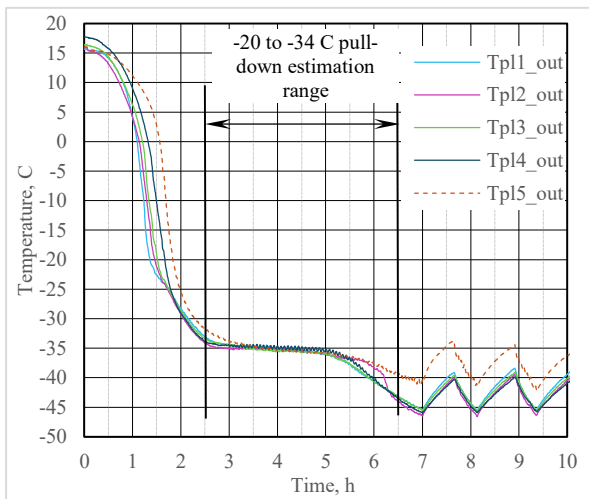


Fig. 8 Eutectic plates temperature near exit during pull-down after defrosting, empty body, ambient temperature 27 oC.

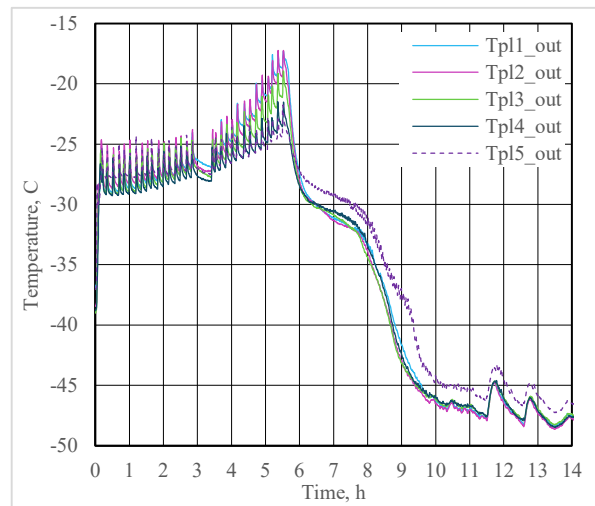


Fig. 9 Temperature of the eutectic plates at the exit during the simulated sales cycle and subsequent pull-down, body loaded with products, ambient temperature 20 C.

5. CONCLUSIONS

A new configuration of eutectic plates introduced in the second eutectic refrigerating system prototype with R1270 refrigerant allowed to reduce the volume of the evaporator by 55% (from 8 to 3.6 l).

Although the refrigerating capacity (and pull-down duration) of both ERS is almost the same, the evaporation temperature increased by 1 K during the crystallization of the eutectic plates in the second prototype.

A new evaporator configuration with eutectic plates connected in parallel and fed through a distributor ensures sufficiently uniform freezing of the eutectic plates in both empty and loaded bodies.

Since our goal in designing the new eutectic plate system was to reduce the volume of the evaporator (and the refrigerant charge), the performance of the new eutectic plate system is better than expected.

NOMENCLATURE

CPRV – crankcase pressure regulating valve	LFL – lower flammability limit
EEV – electronic expansion valve	MOP – maximal operating pressure
ERS – eutectic refrigerating system	PFAS - per- and polyfluoroalkyl substances
GWP – global warming potential	SLHX – suction/liquid heat exchanger

REFERENCES

- Klein, S.A., Reindl, D.T., Brownell, K., 2000. Refrigeration system performance using liquid-suction heat exchangers. *International Journal of Refrigeration*. 23, 588-596 [https://doi.org/10.1016/S0140-7007\(00\)00008-6](https://doi.org/10.1016/S0140-7007(00)00008-6)
- Lemmon, E.W., Huber, M.L., McLinden, M.O., 2018. NIST Standard Reference Database 23: Reference Fluid Thermodynamic and Transport Properties-REFPROP, Version 10.0. National Institute of Standards and Technology, Standard Reference Data Program, Gaithersburg, MD, USA.
- Quibén, J.M., Thome, J.R., 2007. Flow pattern based two-phase frictional pressure drop model for horizontal tubes. Part I: Diabatic and adiabatic experimental study. *International Journal of Heat and Fluid Flow*. 28, 1049-1059 <https://doi.org/10.1016/j.ijheatfluidflow.2007.01.003>
- Quibén, J.M., Thome, J.R., 2007. Flow pattern based two-phase frictional pressure drop model for horizontal tubes, Part II: New phenomenological model. *International Journal of Heat and Fluid Flow*. 28, 1060-1072 <https://doi.org/10.1016/j.ijheatfluidflow.2007.01.004>
- Steiner, D., 1993. Heat transfer to boiling saturated liquids, in: VDI-Warmeatlas (VDI Heat Atlas), Verein Deutscher Ingenieure, VDI-Gesellschaft Verfahrenstechnik und Chemie-ingenieurwesen (GCV), Dusseldorf, (Translator: J.W. Fullarton).
- Vaitkus, L., Balčius, A., 2022. Low GWP drop-in alternative refrigerants for low-temperature transport refrigerators with eutectic refrigerating systems. 7th IIR International Conference on Sustainability and the Cold Chain. <https://doi.org/10.18462/iir.iccc2022.1121>.
- Vaitkus, L., Dagilis, V., 2014. Refrigerant charge reduction in low-temperature transport refrigerator with the eutectic plate evaporator, *Int J Refrigeration*. 47, 46–57. <https://doi.org/10.1016/j.ijrefrig.2014.07.011>.
- Vaitkus, L., Dagilis, V., 2017a. Analysis of alternatives to high GWP refrigerants for eutectic refrigerating systems. *Int J Refrigeration*. 76, 160-169. <https://doi.org/10.1016/j.ijrefrig.2017.01.024>.
- Vaitkus, L., Dagilis, V., 2017b. Experimental investigation of transport refrigerator with eutectic plate evaporator and economizer with intermediate heat exchanger. *Mechanics*. 23 (1), 62-69. <https://doi.org/10.5755/j01.mech.23.1.14319>
- Vaitkus, L., Prakopavičius, L., Balčius, A., 2024. Refrigerants for eutectic refrigerating systems - experimental results and future consideration. *Int J Refrigeration*. In press. <https://doi.org/10.1016/j.ijrefrig.2024.04.012>
- Wojtan, L., Ursenbacher, T., Thome, J.R., 2005. Investigation of flow boiling in horizontal tubes: Part I—A new diabatic two-phase flow pattern map. *International Journal of Heat and Mass Transfer*. 48, 2955–2969 <https://doi.org/10.1016/j.ijheatmasstransfer.2004.12.012>
- Wojtan, L., Ursenbacher, T., Thome, J.R., 2005. Investigation of flow boiling in horizontal tubes: Part II - Development of a new heat transfer model for stratified-wavy, dryout and mist flow regimes. *International Journal of Heat and Mass Transfer*. 48, 2970–2985 <https://doi.org/10.1016/j.ijheatmasstransfer.2004.12.013>